Waste Management 181 (2024) 11–19

Contents lists available at ScienceDirect

Waste Management

journal homepage: www.elsevier.com/locate/wasman

Research Paper

Pressurized pyrolysis of mattress residue: An alternative to landfill management

Daniel Serrano [a,*], Alen Horvat [a], Ricardo M. Mata [b], Paula Costa [b], Filipe Paraleda [b]

[a] Energy System Engineering Research Group, Thermal and Fluid Engineering Department, Carlos III University of Madrid, Leganés, Madrid, Spain
[b] LNEG – National Laboratory on Energy and Geology, Estrada do Paço do Lumiar, Lisbon, Portugal

ARTICLE INFO

Keywords:
Mattress
Waste valorization
Pyrolysis
Waste-to-energy

ABSTRACT

Mattresses are a difficult waste to manage in landfills due to their large volume and low density. Pyrolysis treatment could reduce its volume while producing fuel or products valuable for the chemical industry. Pressurized pyrolysis at 400, 450, and 500 °C is carried out in a lab-scale autoclave at initial pressures 4.2, 8.4, and 16.8 bar. Product gas yield increases slightly along with elevated pressure as well as temperature. However, beyond 8.4 bar the initial pressure makes no discernible differences. CO and CO_2 are the major gas species followed by CH_4. CO contributes the most to the product gas energy content followed by C_3 species, C_2H_6, and H_2. Calculated energy content (heating value) is between 2 and 15 $MJ{\cdot}Nm^{-3}$. In terms of product gas energy content, low pressure pyrolysis is favorable over high pressure pyrolysis. According to integration areas of chromatographic measurements the liquid phase contains up to 25 % of N-compounds, with benzonitrile being the most abundant, followed by toluene, o-xylene, and ethylbenzene. The solid char maintains constant properties across operating conditions, with carbon and energy contents of approximately 75 wt% and 30 $MJ{\cdot}kg^{-1}$, respectively.

1. Introduction

The dream of the perfect mattress is fuelling a consumer boom. Sleep economy grows, as online companies offer 100-day free returns. Along with the old/worn mattresses, about 20 % return rates mean that those are also going to be potentially wasted (Kale, 2020). In Europe, around 30 million mattresses are retired every year (Veses et al., 2021), facing difficult end-of-life management due to large volume (i.e., up to 650 L per mattress), products' mechanical durability, and low density (Garrido et al., 2017). 60 % of the waste mattresses are sent to landfill while 40 % are incinerated (Garrido et al., 2016a, 2016b). In the landfill operations, this bulky waste causes damage to landfill equipment, creates underground voids allowing explosive CH_4 gas to accumulate, and takes decades to decompose, polluting soil and groundwater. According to the Directive (EU) 2018/851 materials recovery and recycling are preferential waste management strategies. However, certain waste is difficult to recycle. Mattresses are of multi-material composition made of four principal materials (i) textile, (ii) foam, (iii) metal, and (iv) wood. The proportion of principal materials depends on the mattress type, either with a metal spring or foam in the core. Griffiths et al. (Griffiths et al., 2013) estimated that a typical disposed mattress contains 30 – 45 wt% of steel spring assembly while the rest accounts for 55 – 70 wt% of the total mass. Disassembling a mattress is challenging and labor-intensive which makes recycling less economically viable. Disassembly methods are usually manual or automated, although the latter gets complicated if the mattress contains staples/stitching/buttons that serve for fixation of upper layers to spring assembly. Although there are well-defined recycling routes for metal springs it is hard to find takers for the foam and textile (Griffiths et al., 2013). Synthetic textile is a blend of strong fibers difficult to "open" and sort out into distinct materials (Hawley, 2014). Along with that, textile and foam maybe biologically contaminated by human and animal secretions. Thus, recovered materials for which a secondary market does not exist can be utilized in an energy recovery processes as the only viable disposal strategy. Incineration reduces the volume of the waste but it may be hindered by the presence of flame retardants in the foam and textile (i.e., CFCs). Zia et al. (Zia et al., 2007) reviewed and discussed chemical or thermochemical methods (waste-to-energy) as a feasible approach for the disposal of scrap polyurethane (PU) foam.

The measured calorific value of non-metal material is in the range of 18.5 to 23.8 $MJ{\cdot}kg^{-1}$, which is suitable for energy applications. Volatile matter is high (68.7 wt% to 86.6 wt%), moisture content varies from 1.3 wt% to 9.5 wt%, while ash content is 1.0 wt% or lower. However,

* Corresponding author.
E-mail address: daserran@ing.uc3m.es (D. Serrano).

https://doi.org/10.1016/j.wasman.2024.03.028
Received 18 December 2023; Received in revised form 5 March 2024; Accepted 25 March 2024
Available online 3 April 2024

Nomenclature

Abbreviations

GC	gas chromatography
FID	flame ionization detector
HHV	higher heating value
LHV	lower heating value
MSD	mass spectrometry detector
PAH	polycyclic aromatic hydrocarbon
PU	polyurethane
TCP	trycresil phosphate

shredded mattress residue may contain moisture above 40 wt%, due to high water adsorption capacity and wet weather exposure at the processing plants. Likewise, the ash content may be relatively high due to slivers of metal trapped in shredded residue (Griffiths et al., 2013). Mattresses include synthetic materials such as polyethers, polyester polyols, methyl diphenyl diisocyanate, and toluene diisocyanate (Chattopadhyay and Webster, 2009). The nitrogen (N) content in these materials may be up to 150 times that in biomass, making incineration unfavorable owing to pollutant gas emissions (i.e., NO_x, NH_3, and HCN) (Czajczyńska et al., 2017; Garrido et al., 2017). Since the thermochemical conversion in an inert atmosphere reduces NO_x and SO_2 emissions, processes like pyrolysis may be ecologically acceptable (Chen et al., 2014). Mehta and Golkaram (Mehta and Golkaram, 2022) conducted a sustainability analysis on end-of-life treatments of waste mattresses, finding that pyrolysis can save 526 kg CO_2-eq and 5.1 GJ of energy per ton of mattress compared to incineration. Pyrolysis employs moderate temperatures between 300 and 700 °C in an inert atmosphere to produce a solid fraction or char, a gas phase, and a liquid phase or pyrolysis oil. Product distribution depends on the operating conditions such as heating rate and gas residence time. The mattress durability (i.e., well mechanically integrated product) and the flame retardant additives are beneficial along the mattresses lifetime, but could affect the processes after their life has ended. (Zia et al., 2007). Several contemporary authors reported that the addition of flame retardants improved thermal degradation up to a certain extent. Wang et al. (Wang et al., 1999) studied thermal degradation of PU by the thermogravimetric analysis in an inert atmosphere. Degradation occurred in two stages. The presence of flame retardant led to a decrease of the activation energy in the first stage, but an increase in the second stage. The increase of the activation energy was attributed to the formation of a thermally stable structure. PU containing flame retardant produced higher char yield than the plain PU. Chen et al. (Chen et al., 2013) employed thermogravimetric analysis-infrared spectrometry to study PU containing tricresyl phosphate (TCP) as a flame retardant. PU containing a high portion of TCP exhibited relatively low thermal stability at low temperature due to the lower stability of P-O-C bonds compared to common C–C bonds. However, thermal stability increased at elevated temperature along with higher char formation compared to PU containing a low portion of TCP. Measurements also showed that TCP flame retardant reduces combustible gas products and reduces the toxic gases containing NCO groups while non-flamable CO_2 increase. Furthermore, the comprehensive review compiled by Zakharyan and Maksimov (Zakharyan and Maksimov, 2022) indicated that the type of isocyanates (most common, 4,4′-methylene diphenyl diisocyanate and toluene diisocyanate), polyols additives such as chain extenders, flame retardants, crosslinking agents, foaming agents, and catalysts utilized during PU synthesis have an effect on the pyrolysis products.

Mattress pyrolysis trials have been carried out previously, but using solely PU foams as a feedstock because these are the main materials in the mattress composition. Various authors conducted kinetic studies (Garrido et al., 2016b; Jiang et al., 2021; Wan and Huang, 2022; Zhang et al., 2009a, 2009b), observing different decomposition steps, the first of which produces cyanates, amines, CO_2 and a condensable phase from the cleavage of urethane bonds. In the second step, condensable phase is degraded into aliphatic and aromatic hydrocarbons, ethers and polyols. Veses et al. (Veses et al., 2021) combined pyrolysis together with thermal/catalytic cracking process at different temperatures, obtaining moderate amounts of H_2 in the product gas. The use of dolomite, olivine, or Ni-based catalysts promoted the gas phase yield at the expense of the liquid phase. Several authors investigated hazardous emissions from N-derived chemicals during PU pyrolysis and combustion (Adeosun, 2014; Garrido et al., 2017, 2016a; Guo et al., 2014). Garrido et al. (Garrido et al., 2017, 2016a) used lab-scale pyrolysis and combustion facility to study N-compounds, light hydrocarbons, polycyclic aromatic hydrocarbons (PAHs), and chlorinated aromatics (ClBzns, ClPhs, PCDD/Fs, and dlPCBs). Light N-compounds such as HCN, NH_3, and NO were released during thermochemical conversion, although pyrolysis produced less of those compared to combustion. However, increasing pyrolysis temperature enhanced the formation of HCN, NH_3, and nitrile compounds. Temperature increased the toxicity of PAHs as a consequence of higher benzo(a)pyrene yield. PCDD/Fs also increased with temperature due to H-radicals, which open and activate the N-containing heteroaromatic ring systems (Li and Tan, 2000).

Although the number of studies did address valorization of mattress via pyrolysis, none has been done on the entire mattress as received by the municipal solid waste company. The novelty of the current study is to evaluate pressurized pyrolysis of real mattress waste containing diverse chemical make-up of PU foams, fabrics, and textiles, as well as to analyse pryolysis product distribution and composition. The significance of this work is the contribution to the following four points: (1) waste management: diverting mattresses from landfills; (2) resource recovery: pyrolysis products can reduce the demand for virgin resources; (3) circular economy: the study is aligned with principles of a circular economy by reuse of materials; and (4) environmental benefits: reduction of greenhouse gas emissions and leaching of contaminants into water strams, compared to traditional waste disposal methods.

2. Experimental setup

2.1. Materials

Mattress waste provided by waste collection enterprise LYMA Getafe is used as feedstock. Industrial shredder is used to break down the mattress into small pieces (Fig. 1). In this process, metal parts are removed by magnets. Shredded residue is fully characterized by elemental, proximal, and higher and lower heating value (HHV, LHV)

Fig. 1. Shredded mattress waste residue.

analyses according to the standards ISO 16948, CEN/TS 15414–1:2010, ISO 21656:2021, ISO 22167:2021, and ISO 18125. The feedstock characterization in Table 1 shows a high volatile content and a low moisture content. The latter may vary because the waste treatment enterprise shreds and stores waste residue in open-air facilities. Table 1 also shows the elemental composition in relation to data from the literature. In terms of volatile content and fixed carbon, the entire mattress waste used in this study is comparable to the wadding material and synthetic foam used by Griffiths et al. (Griffiths et al., 2013), suggesting that these are the main materials in mattress make up. Eschenbacher et al. (Eschenbacher et al., 2021) reported similar values of volatiles and fixed carbon for different types of PU foams. The wadding and textile fibre may be the cause of the variations in these values from those reported by Garrido et al. (Garrido et al., 2017, 2016b) and Veses et al. (Veses et al., 2021), who only used PU foams. The elemental analysis results, however, do not significantly differ, suggesting material homogeneity (Garrido et al., 2017; Griffiths et al., 2013; Veses et al., 2021).

2.2. Experimental facility and procedure

Mattress waste residue is pyrolyzed in a 1 dm^3 Hastelloy C276 autoclave (Parr Instruments). The autoclave is electrically heated and equipped with stirring blades and a cooling pipe. The target temperature is set using a controller device, while the reaction temperature, pressure, and stirring velocity of the feedstock are monitored. The experimental setup is depicted in Fig. 2.

Closed reactor is loaded with 22 g of shredded mattress waste residue. The reactor vessel is then flushed three times with N_2 to create an inert atmosphere. Following the flushing, the reactor is ultimately pressurized with N_2 to a selected initial value. The reactor is then heated to the reaction temperature. As indicated in Table 2, three different reaction temperatures (400, 450, and 500 °C) and initial pressures (4.2, 8.4, and 16.8 bar) are tested. Selected operating conditions are limited by the maximal operation temperature and the maximal pressure at which the autoclave withstands leaks. Due to reactor limitations only 400 and 450 °C are tested at the highest initial pressure. Once the reaction temperature is attained, the pyrolysis reaction is held for 30 min. The reaction temperature and reaction pressure shown in Table 2 refer to the mean values during 30 min test. At the end of this period, the system is promptly cooled to the ambient temperature, using water flow through a cooling pipe inside the reactor vessel.

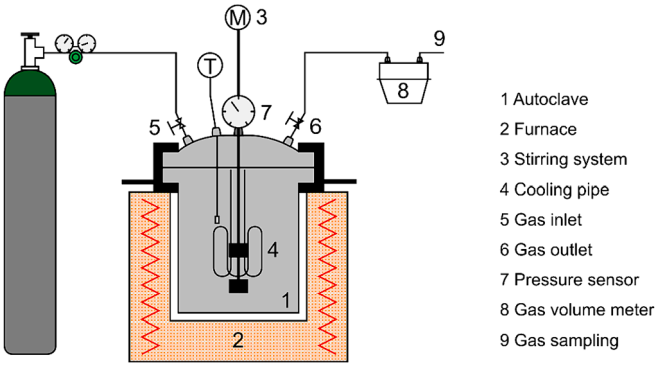

Fig. 2. Schematic diagram of the autoclave pyrolysis installation.

2.3. Sampling and analysis

When the reactor cools down to ambient temperature, 31 °C, the gases are measured with a gas volume meter (Elster BK-G4) and sampled into a gas bag for chromatographic analysis. The autoclave is then opened, collecting the liquid and solid phases from the reactor, weighing, and kept for analysis. Actually, no liquid phase is obtained directly. Minor amount of produced liquid is found on the reactor's lid and walls, as well as the sealing gasket, and cooling pipe. These amounts are to small for complete quantitative sampling of the liquid phase. Instead, the surfaces holding droplets of produced liquid are washed with 60 cm^3 of 2-propanol in order to perform qualitative characterization of the liquid phase.

Collected solid phase is subjected to a Soxhlet extraction because solids absorb produced liquid. 3 g of solid sample are placed in the extraction filter. Each solid-filled filter is then immersed in 50 cm^3 of n-hexane for 3 h at 140 °C. After that, the filter is removed from the n-hexane, dripping for 1 h. Finally, n-hexane evaporation from the solid phase is carried out at 50 °C until the solid reaches a constant weight. Dry solid samples are analysed by proximate, elemental analysis, HHV, and LHV (Table 2).

The gas samples are analyzed using Hewlett Packard 6890 gas chromatography (GC) equipment with two columns and two detectors.

Table 1
Characterization of mattress waste residue and comparison with literature data.

	This study	(Griffiths et al., 2013)					(Garrido et al., 2016b)†	(Garrido et al., 2017)†	(Veses et al., 2021)†
Feedstock	Complete mattress waste	Wadding	Natural fibre	Synthetic foam	Felt	Fluff residue	Flexible polyurethane foam (FPUF)	Viscolastic memory foam (VMF)	Mattress foam
Proximate analysis [wt.%]$_{ar}$									
Moisture	3.6 ± 0.6	1.3	9.5	2.9	5.0	44.9		1.3	
Volatile	81.4 ± 1.5	86.6	68.7	84.6	74.5	45.9		99.7	98.2
Fixed Carbon[a]	12.3	11.5	20.7	12.4	19.5	5.6			0.8
Ash	2.7 ± 0.4	0.6	1.0	0.2	0.9	3.6	5.5	0.11	1.0
Elemental analysis [wt.%]$_{db}$									
Carbon	62.7						57.8	61.3	62.2
Hydrogen	7.2						7.4	8.4	8.6
Nitrogen	3.9						5.9	3.3	6.8
Sulfur	0.3						<0.01	0.2	0.3
Chlorine	0.3								
Oxygen[a]	22.8						23.4	26.7	23.1
Higher Heating Value [MJ·kg^{-1}]$_{ar}$	26.5								
Lower Heating Value [MJ·kg^{-1}]$_{ar}$	24.9						24.2	27.1	27.3

ar: as received, db: dry basis, [a] determined by difference.
† no indication about the analysis basis.

Table 2
Operating conditions and characterization of solid char.

	#01	#02	#03	#04	#05	#06	#07	#08	Mean value ± standard deviation
Operating conditions									
Initial pressure [bar]	4.2	4.3	4.2	8.4	8.4	8.3	16.8	16.8	
N_2 volume [Ndm^3]	4.2	4.3	4.2	8.5	8.5	8.4	17.0	17.0	
Reaction temperature† [°C]	402	443	503	400	449	503	402	450	
Reaction pressure† [bar]	26.0	32.8	37.8	35.4	39.6	41.1	51.0	60.7	
Proximate analysis [wt.%]$_{ar}$									
Moisture	3.0	3.2	2.7	3.4	2.9	3.0	3.3	3.0	3.1 ± 0.2
Ash	7.5	6.0	9.9	6.6	7.8	7.8	6.6	6.4	7.3 ± 1.2
Elemental analysis[a] [wt.%]$_{db}$									
Carbon	74.3	75.7	78.7	74.2	75.9	77.6	76.3	76.5	76.2 ± 1.5
Hydrogen	2.9	2.4	2.4	2.8	2.4	2.0	3.7	2.6	2.7 ± 0.5
Nitrogen	9.5	10.8	7.8	10.4	9.2	8.3	8.4	9.0	9.2 ± 1.0
Sulfur	≤ 0.2	≤ 0.2	0.4	≤ 0.2	≤ 0.2	≤ 0.2	0.5	≤ 0.2	
Heating value [MJ·kg^{-1}]$_{ar}$									
HHV	30.0	29.9	29.7	32.5	30.0	30.2	32.0	30.5	30.6 ± 1.1
LHV	29.4	29.4	29.2	31.9	29.5	29.8	31.2	29.88	30.0 ± 1.0

ar: as received, db: dry basis, [a] oxygen determined by difference.
† mean value during 30 min test.

A molecular sieve 5A (MS5A) column and a Porapak Q (PPQ) column linked to a thermal conductivity detector (TCD) and a flame ionization detector (FID) connected in series are used to measure H_2, CO_2, CO, and hydrocarbons ranging from CH_4 to C_4H_{10}. Argon is employed as the carrier gas. The GC oven program starts at an isothermal stage of 40 °C for 17 min, followed by a 15 °C·min^{-1} ramp up to 185 °C, and ending with an isothermal stage for 43 min. GC detectors are linearly calibrated for every gas compound at various concentration levels. In the event of identified hydrocarbons larger than C_4, the calibration curve for n-C_4H_{10} is employed.

The liquid phase is analyzed by an Agilent 8890 GC equipped with a 5977B GC/MSD and an Agilent DB-5 ms 30 m x 250 µm x 0.25 µm capillary column. Helium is used as a carrier gas at a flow rate 1 ml·min^{-1}. The injector temperature is set to 250 °C at a 8.2 psi pressure and a 10:1 injection split mode. The GC oven initiated at 60 °C, with a heating ramp of 15 °C·min^{-1} up to 100 °C, then 25 °C·min^{-1} up to 260 °C with a hold period of 15 min, and finally 25 °C·min^{-1} up to 300 °C with a hold time of 5 min. The temperatures of the mass spectrometer (MSD) transfer line, ion source, and quadrupole mass analyzer are set at 250, 230, and 150 °C, respectively. During the first 7 min of the method, the MSD is configured to scan molecular masses from 10 to 250 *m/z*, and from 40 to 340 *m/z* for the remaining time of the analysis. The NIST 23 library is used to identify liquid compounds.

The weight difference is used to calculate yields of the three product fractions (i.e., gas, liquid, solid). The weight of wet solids collected from the reactor and the amount of dry solid residue recovered following Soxhlet extraction are used to calculate solids. The amount of liquid is calculated by summing up the weight difference of the reactor vessel after the experiment (wet solid plus liquid on the reactor surface) and the wet solid, plus the amount of liquid recovered from the wet solids. Finally, the amount of gas is computed by difference.

3. Results and discussion

3.1. Product yields

Fig. 3 depicts the product distribution achieved in the pyrolysis process. The solid (char) generation remains almost constant with respect to temperature and pressure, resulting in a mean value of 30.2 ± 1.5 wt%. Jomaa et al. (Jomaa et al., 2015) reported similar values, 26.7 wt%, for PU degradation between 200 and 1000 °C, where half of the weight loss occurred below 300 °C due to polyol and polyisocyanate bonds dissociation (first devolatilization stage). Higher devolatilization compared to the present study could be due to the more severe thermal conditions. Veses et al. (Veses et al., 2021) obtained a lower yield of solid phase, around 7.6 wt% depending on the cracking temperature. In the current study, mattress residue undergoes a slow pyrolysis process in which the feedstock is slowly heated up until the reaction temperature is reached. Generated gases remain at that temperature for an extended period of time, compared to fast pyrolysis and post-treatment conditions carried out by Veses et al. Furthermore, other studies tested only PU foam material as a pyrolysis feedstock, resulting in a greater concentration of volatiles, close to 99 wt% (Garrido et al., 2017, 2016b; Veses et al., 2021). The mattress waste residue employed in this study also includes fabric stripes and coverings, as well as thin fibers, resulting in a reduced volatile content and higher fixed carbon and ash content (Table 1). In addition, the presence of flame retardants in the feedstocks used in all these studies could also affect to the charring process (Eschenbacher et al., 2021).

The temperature variations affect the yield of liquid. With the

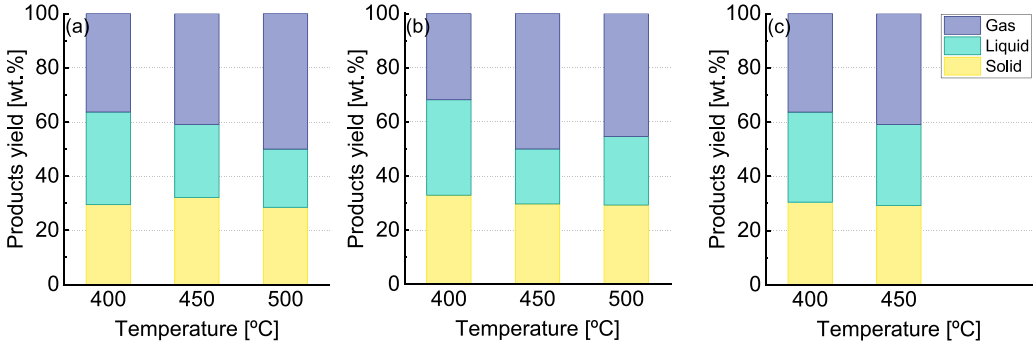

Fig. 3. Product distribution as a function of initial pressure: a) 4.2 bar, b) 8.4 bar, and c) 16.8 bar, and reaction temperature.

increasing temperature, the yield of liquid decreases from around 34 to 21 wt%. The effect of pressure on the yield of liquid is minor at 400 and 500 °C, with maximal variations of 3.1 and 3.8 wt%, respectively. At 450 °C, the variations reach up to 9.6 wt% from 8.4 to 16.8 bar, although this difference is only 2.9 wt% between 4.2 and 16.8 bar. In these conditions, a decrease in the liquid amount is mainly accompanied by an increase in gas yield and a marginal reduction in the solid fraction. The distribution of products at initial pressures 4.2 and 8.4 bar at 450 and 500 °C is similar. In these two cases, the highest amount of gas, approximately 50 wt%, is produced. This value could be increased by further raise of the reaction temperature (Veses et al., 2021).

3.2. Gas phase

Prior to the experimental test, the initial pressure is adjusted by the amount of N_2 introduced into the reactor. This causes dilution of the product gas, and, consequently affects its composition in terms of absolute values. Therefore, the results are expressed on a N_2-free basis to facilitate comparison.

Fig. 4 depicts the gas species measured in the product gas. The main compounds are CO and CO_2, showing the presence of O-containing polymers (e.g., polyesters and PU) in the feedstock, as expected for this type of residue. Thermal breakdown of PU generates primary and secondary amines, olefins, and CO_2 (Ketata et al., 2005; Zhang et al., 2009b). CH_4, is also present in significant amounts, particularly at higher temperatures.. Garrido et al. (Garrido et al., 2017) and Veses

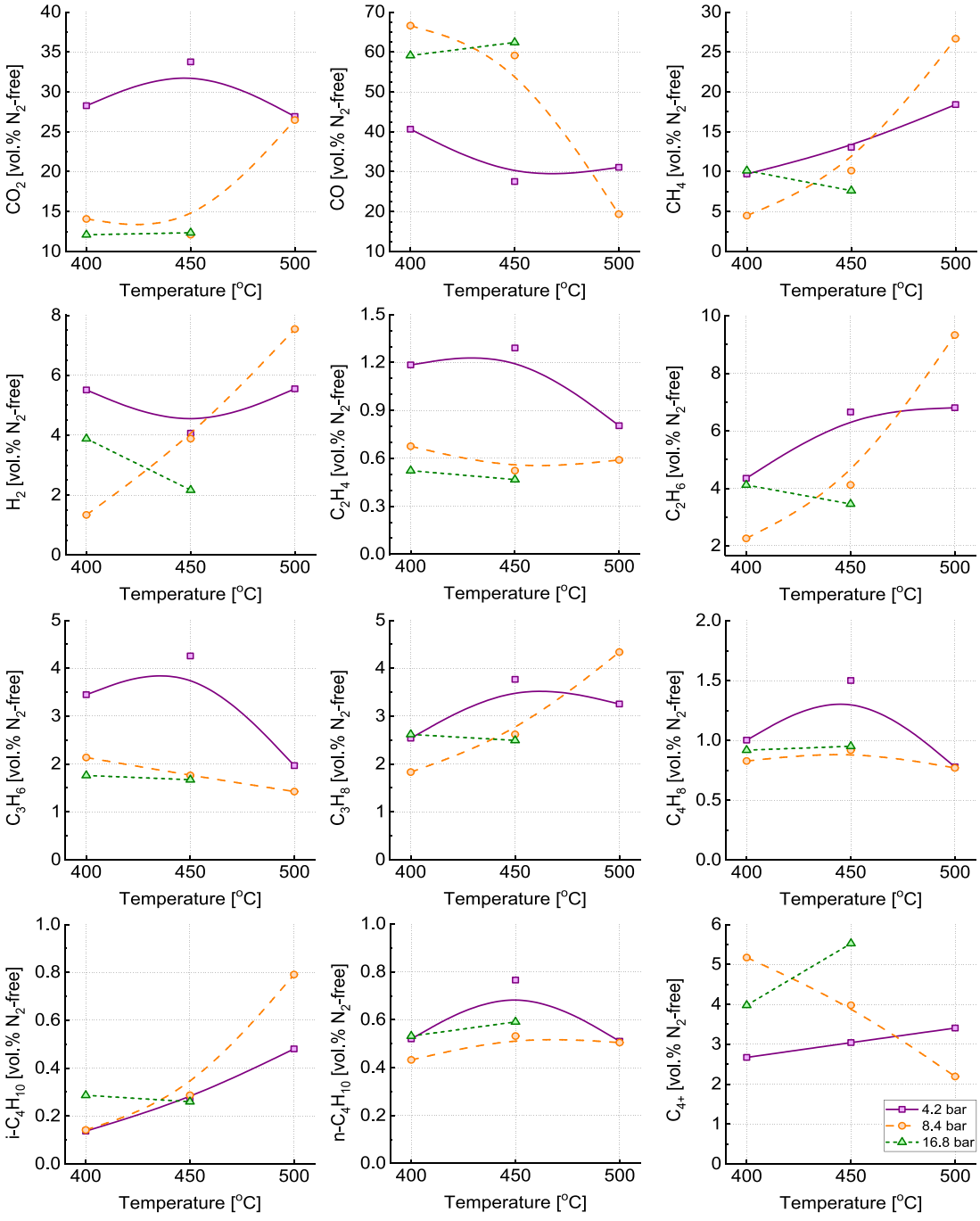

Fig. 4. Volumetric concentration of gas species in the product gas (lines indicate trends rather than regression).

et al. (Veses et al., 2021) also measured large amounts of CH_4 and C_2 light hydrocarbons, in some cases those values were substantially greater than CO, CO_2, and H_2. The amount of C_3 species is notable. The sum of C_3 species is comparable to H_2 content and C_2 species. The formation of C_3 species is linked to the simultaneous breakdown of urethane, polyether, and aliphatic oxygenated functional groups present in the feedstock (Adeosun, 2014). The significant yield of C_2 and C_3 species (i.e., C_2H_4 and C_3H_6) is of great interest for the petrochemical industry, opening the possibility to chemically recover monomers from the raw product gas. This novel chemical recycling is still a premature technology, but has a potential to be part of supply chain for new high-quality plastics (Abbas-Abadi et al., 2023). Several C_4 species are also produced but in quantities of 1 vol% or below. Finally, up to 12 unknown gas species heavier than C_4 are detected. They are classified as C_{4+} compounds. The total amount of C_{4+} compounds accounts for 2 – 5 vol%, having a significant impact on the product gas. Serrano et al. (Serrano et al., 2022) reported how C_{4+} and longer hydrocarbons chains affect the energy content of the product gas with differences bigger than 50 % if they are not considered. Thus, the determination of all gas species makes an important improvement in the pyrolysis product gas.

The initial pressure has a notable effect on the gas composition. At the temperatures 400 and 450 °C, elevated initial pressure causes a decrease in all gas species except CO and C_{4+} compounds. The variations between the highest and lowest content reach 114 % for CO, 76 % for H_2, and 64 % for CO_2. However, the initial pressure of 16.8 bar has a lesser effect compared to the initial pressure 8.4 bar against 4.2 bar. At low initial pressure of 4.2 bar the effect of temperature is not substantial. CO concentration reduces by 13 vol% while compounds such as CH_4, C_2H_6, i-C_4H_{10}, and C_{4+} experience a modest increase in quantity as a result of pyrosynthesis reactions promoted by an elevated temperature (Garrido et al., 2016a) and the breakage of chemical bonds in the feedstock polymer structure (Niu et al., 2023). At intermediate initial pressure of 8.4 bar, a strong temperature effect is observed for H_2, CO_2, CH_4, CO, and C_2H_6. For example, measurement shows that between 400 and 500 °C CO yield reduces by 47 vol%. The findings of the current study are not in the line with those obtained by Veses et al. (Veses et al., 2021) and Wang et al. (Wang et al., 2017). Veses et al. conducted pyrolysis of mattress foam at 550 °C followed by mineral catalyst assisted thermal cracking at 800 °C. Authors reported that CO increased production is due to Boudouard reaction ($C + CO_2 \leftrightarrow 2CO$) and dry reforming reaction ($C_nH_m + nCO_2 \leftrightarrow 2nCO + (m/2)H_2$). Wang et al. tested municipal solid waste pyrolysis at 500 °C followed by thermal cracking at 600 °C in the presence of char. Authors did not observed a notable change in the concentration of CO during the test campaing. Garrido et al. (Garrido et al., 2017) alluded to an increase in both CO_2 and CO with increasing temperature.

The N_2 dilution caused by the initial pressure setting impacts the energy content of the product gas. The energy content is estimated in terms of the LHV (Basu, 2010) and displayed in Fig. 5a, using the data of raw product gas composition (including added N_2). Fig. 4 shows that the quantity of combustible gas species is greater at the lowest pressure level, resulting in a higher LHV gas. Low-pressure conditions are favorable since the product gas contains 45 to 52 % more energy than high-pressure condition. LHV at high-pressure, 16.8 bar, remains unchanged with respect to the intermediate initial pressure of 8.4 bar. In case LHV is presented on a N_2-free basis to eliminate the effect of the gas dilution, higher pressures produce a product gas with a higher LHV, 24.2 vs, 21.5 MJ·Nm^{-3}, at 400 °C. This trend is reversed at 500 °C, where the LHV for an initial pressure of 4.2 bar is 28.7 MJ·Nm^{-3} while for an initial pressure of 8.4 bar LHV results 24.8 MJ·Nm^{-3} (see Supplementary Material). CO is the gas species that contributes the most to the energy content of pyrolysis product gas across all pressure settings as a consequence of the yield and energy content per Nm^3, followed by C_{4+}, CH_4, C_2 and C_3 compounds. Fig. 5b shows the contribution of each gas compound to LHV taking data from pyrolysis at temperature 400 °C (see Supplementary Material for 450 and 500 °C).

The energy content of product gas is rather low, between 2 and 15 MJ·Nm^{-3}. For comparison, Veses et al. (Veses et al., 2021) reported values up to 33 MJ·Nm^{-3} for non-catalytic pyrolysis of mattress foams. High LHV values were attributed to C_1-C_4 hydrocarbons produced at the low temperature (350 °C) non-catalytic thermal cracking. Under catalytic (dolomite, olivine, and HiFUEL® R110) and non-catalytic conversions at high cracking temperatures of 800 °C LHV values of approximately 18 MJ·Nm^{-3} were obtained. Authors reported LHV values on a N_2-free basis (Veses et al., 2021). Nonetheless, the gas produced in this study can be used to generate energy by burning it in a gas turbine, a boiler for a Rankine steam power cycle, or in an internal combustion engine (Shudo et al., 2003). Other product gas applications, such as chemicals or H_2 production will require additional and non-trivial process improvements. Chemical vapor deposition can be the approach to produce carbon nanotubes from the mix of hydrocarbon gases (C_1 – C_4) and high H_2 concentration obtained from pyrolysis processes. Veksha et al. (Veksha et al., 2023, 2022) demonstrated the feasibility of this approach converting polyolefin plastics into small diameter carbon nanotubes. These new applications and synergies between technologies will improve the reuse and recycling of materials into new products, mitigating unsustainable extraction of natural resources.

3.3. Solid phase

Table 2 displays the characterization of the solid char. The standard deviation between solid samples is negligible. Due to the low ash level in the feedstock, the ash content in the solid char remains low (7 wt% approx.), while the carbon content remains over 75 wt%, resulting a LHV of 30 MJ·kg^{-1}. These values contradict the findings of Veses et al. (Veses et al., 2021), who reported a char with high ash (43.1 wt%) and low carbon content (36.2 wt%), respectively, and thus, a lower LHV

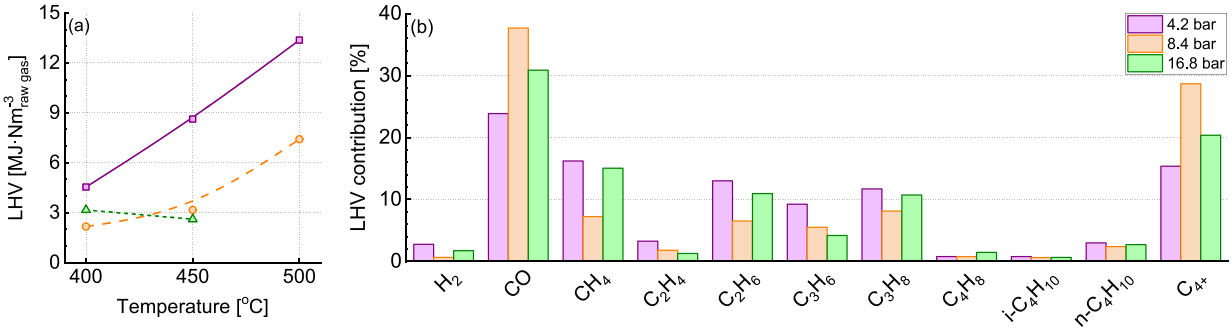

Fig. 5. Energy content of raw product gas: a) LHV at different operating conditions and b) contribution of each gas compound to LHV at 400 °C (See Supplementary data for 450 and 500 °C).

(12.8 MJ·kg^{-1}). Authors attributed their findings to efficient devolatilization of mattress foam at 550 °C. On the one hand, solid char can provide the energy required for pyrolysis process, as energy demand is a crucial factor in terms of environmental sustainability of the process (Batuecas et al., 2023). On the other hand, a high carbon and energy content could indicate inefficient devolatilization (Veses et al., 2021). The setback of low pyrolysis temperature is a solid char with high nitrogen content (Chen et al., 2012).

3.4. Liquid phase

Total ion current chromatograms obtained from the GC/MSD analysis of the liquid fraction recovered (by Soxhlet extraction) from the solid phase produced at 400 °C are shown in Fig. 6. The chromatograms only include compounds with a relative integration area higher than 1 % (see Supplementary Material for chromatograms obtained from pyrolysis tests at 450 and 500 °C).

According to the qualitative analysis, benzonitrile is the most abundant compound. Garrido et al. (Garrido et al., 2016a) also observed benzonitrile as the major semi-volatile compound produced during the thermal degradation of PU. Thermochemical reforming of the urethane bond of the polymer structure is responsible for the production of benzonitrile and its substituted derivatives (Zakharyan and Maksimov, 2022). Toluene, o-xylene, ethylbenzene, and 4-methyl-benzonitrile are also present in all test conditions with a notable chromatographic integration area. At 4.2 and 8.4 bar of initial pressure, these compounds show a decreasing tendency with temperature. They do, however, rise considerably from 400 to 450 °C at 16.8 bar. Actually, production of most of the liquid species increases with the temperature at the highest initial pressure condition. On the other hand, some compounds are only detected at low pressures (e.g., heptadecane, hexadecanenitrile), others only appear at high pressures (e.g., naphthalene, 2,7-dimethyl-). Nearly 60 % of the identified compounds only appear in one experimental condition. This could be attributed to the different polymer make-up of PU foams (Zakharyan and Maksimov, 2022) and diverse textile chemistry in the feedstock. In this study, control over the feedstock composition is not possible since waste mattresses are collected from the wider city area and shredded randomly.

Poor liquid quality from polyurethane foams containing a significant number of N-compounds and polycyclic aromatic hydrocarbons (PAHs) have been reported previously (Garrido et al., 2016a; Veses et al., 2021). In the current study, 90 N-compounds are identified in total (see Supplementary data). From 14 to 31 N-compounds are identified for each operating condition. Their contribution to total integration area ranges

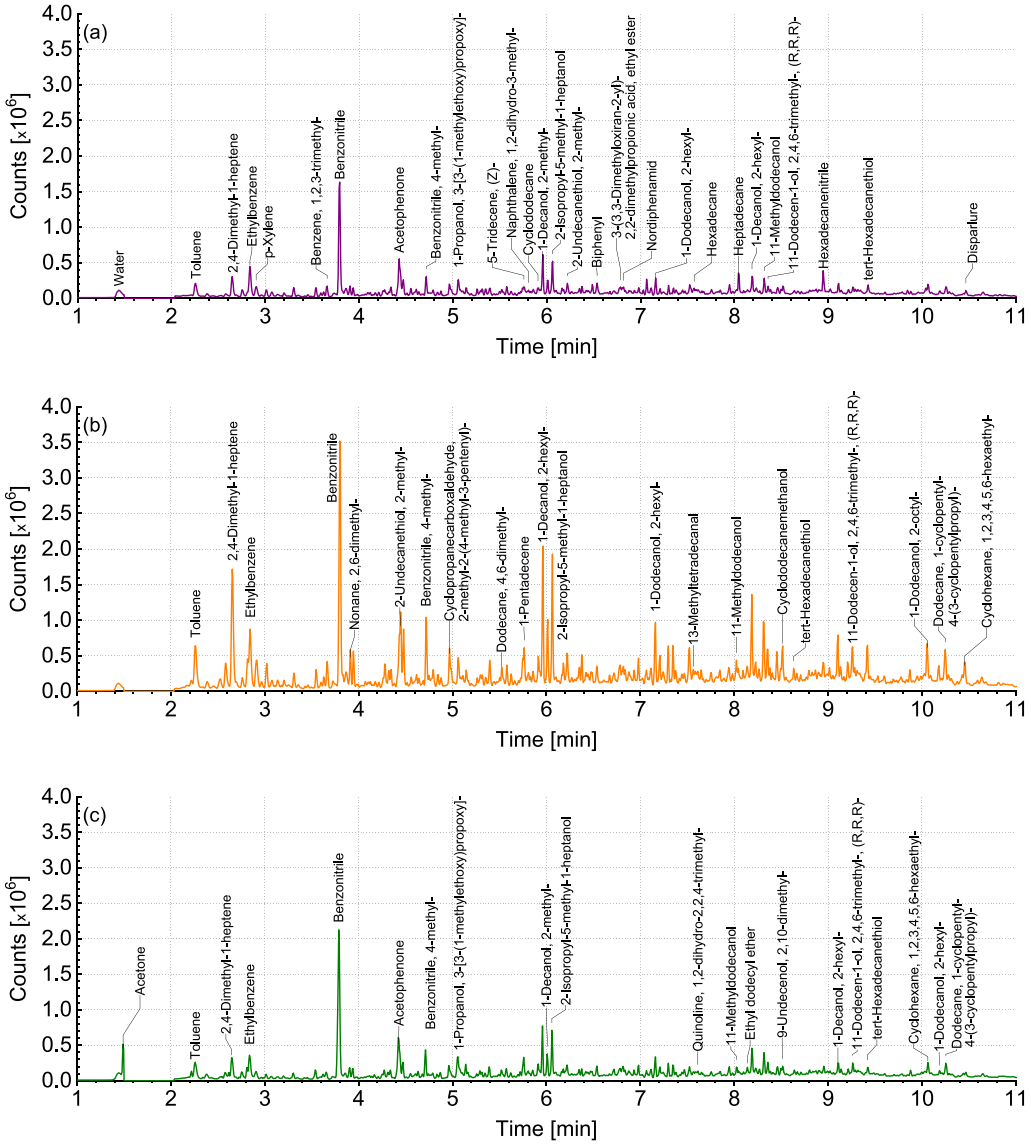

Fig. 6. Total ion current (GC/MSD) chromatograms from Soxhlet extracted liquids produced at 400 °C and a) 4.2 bar, b) 8.4 bar, and c) 16.8 bar.

between 10.3 and 25.7 %. These values are lower than those reported by Guo et al. (Guo et al., 2014) that conducted bench-scale, fixed-bed pyrolysis of waste rigid polyurethane foam at temperatures between 900 and 1100 °C. They measured 19 N-compounds in the liquid phase. Compounds were heterocyclic with nitrile or amine functional groups bonded to aromatic rings. Their contribution to the total integration area was between 39.6 and 47.7 %. The experimental condition at 450 °C produces N-compounds with a higher response in the GC/MSD than the other temperatures at the same pressure level.

4. Conclusions

Waste mattresses call for a solution to prevent large space occupation in landfills. The goal of this research is to investigate waste-to-energy route for real mattress waste containing diverse chemical make-up of PU foams, fabrics, and textiles. Pyrolysis process is performed under various pressurized conditions at 400, 450 and 500 °C.

Properties of solid char remain stable with respect to operating conditions, with constant carbon content and a heating value of approximately 30 $MJ{\cdot}kg^{-1}$. The gas yield is maximal, approximately 50 wt% at initial pressure 4.2 bar and 500 °C or at 8.4 bar and 450 °C, although the latter has lower energy content.

The product gas is predominantly composed of CO and CO_2, which are primarily formed due to polyurethane breakdown, along with CH_4, which increases with temperature and pressure. C_3 compounds are detected in the quantities of several vol.% which is also the case for H_2 and C_2 species. At 400 and 450 °C, the initial pressure has an effect on the product gas composition increasing CO production while decreasing yields of other gas species. Beyond 8.4 bar, further pressure increase has no significant effect. Lower initial pressure produces a raw product gas with higher energy content considering N_2 dilution, with CO being the gas species that contributes the most to the gas energy content across all pressure levels. For N_2-basis, lower initial pressure produces the raw gas with the maximum LHV at 500 °C.

4.2 bar and 500 °C are favorable conditions in terms of gas composition, and thus, energy content of the product gas. These conditions result in low N_2 dilution with moderate concentration of CO_2, and relatively high concentration of other hydrocarbon species.

The most abundant compound in the liquid phase is benzonitrile, followed by toluene, o-xylene, and ethylbenzene. Liquid phase composition is diverse, with only a few of the most abundant compounds being identified in samples across all operating conditions. Mass spectroscopy analysis identified 90 N-compounds in the liquid phase.

CRediT authorship contribution statement

Daniel Serrano: Writing – review & editing, Writing – original draft, Validation, Methodology, Investigation, Conceptualization. **Alen Horvat:** Writing – review & editing, Investigation. **Ricardo M. Mata:** Investigation. **Paula Costa:** Writing – review & editing, Resources, Methodology. **Filipe Paraleda:** Investigation.

Declaration of competing interest

The authors declare that they have no known competing financial interests or personal relationships that could have appeared to influence the work reported in this paper.

Data availability

Data will be made available on request.

Acknowledgements

This research has received funding from the European Union's Horizon 2020 research and innovation programme under grant agreement No 731101 (BRISK II project: Biofuels Research Infrastructure for Sharing Knowledge II). Funding for APC: Universidad Carlos III de Madrid (Read & Publish Agreement CRUE-CSIC 2023).

Appendix A. Supplementary data

Supplementary data to this article can be found online at https://doi.org/10.1016/j.wasman.2024.03.028.

References

Abbas-Abadi, M.S., Ureel, Y., Eschenbacher, A., Vermeire, F.H., Varghese, R.J., Oenema, J., Stefanidis, G.D., Van Geem, K.M., 2023. Challenges and opportunities of light olefin production via thermal and catalytic pyrolysis of end-of-life polyolefins: Towards full recyclability. Prog. Energy Combust. Sci. 96, 101046 https://doi.org/10.1016/J.PECS.2022.101046.

D.O. Adeosun Analysis of fire performance 2014 University of Waterloo Smoke Development and Combustion Gases from Flame Retarded Rigid Polyurethane Foams.

P. Basu Biomass gasification and pyrolysis 2010 Elsevier Inc. Biomass Gasification and Pyrolysis 10.1016/C2009-0-20099-7.

Batuecas, E., Serrano, D., Horvat, A., Abelha, P., 2023. Sustainable conditions for waste tires recycling through gasification in a bubbling fluidized bed. J. Clean. Prod. 415, 137839 https://doi.org/10.1016/j.jclepro.2023.137839.

Chattopadhyay, D.K., Webster, D.C., 2009. Thermal stability and flame retardancy of polyurethanes. Prog. Polym. Sci. 34, 1068–1133. https://doi.org/10.1016/J.PROGPOLYMSCI.2009.06.002.

Chen, X., Huo, L., Jiao, C., Li, S., 2013. TG–FTIR characterization of volatile compounds from flame retardant polyurethane foams materials. J. Anal. Appl. Pyrol. 100, 186–191. https://doi.org/10.1016/j.jaap.2012.12.017.

Chen, H., Wang, Y., Xu, G., Yoshikawa, K., 2012. Fuel-N evolution during the pyrolysis of industrial biomass wastes with high nitrogen content. Energies (basel) 5, 5418–5438. https://doi.org/10.3390/en5125418.

Chen, D., Yin, L., Wang, H., He, P., 2014. Pyrolysis technologies for municipal solid waste: a review. Waste Manag. 34, 2466–2486. https://doi.org/10.1016/J.WASMAN.2014.08.004.

Czajczyńska, D., Anguilano, L., Ghazal, H., Krzyżyńska, R., Reynolds, A.J., Spencer, N., Jouhara, H., 2017. Potential of pyrolysis processes in the waste management sector. Thermal Science and Engineering Progress 3, 171–197. https://doi.org/10.1016/J.TSEP.2017.06.003.

Eschenbacher, A., Varghese, R.J., Weng, J., Van Geem, K.M., 2021. Fast pyrolysis of polyurethanes and polyisocyanurate with and without flame retardant: compounds of interest for chemical recycling. J. Anal. Appl. Pyrol. 160, 105374 https://doi.org/10.1016/J.JAAP.2021.105374.

Garrido, M.A., Font, R., Conesa, J.A., 2016a. Pollutant emissions during the pyrolysis and combustion of flexible polyurethane foam. Waste Manag. 52, 138–146. https://doi.org/10.1016/J.WASMAN.2016.04.007.

Garrido, M.A., Font, R., Conesa, J.A., 2016b. Kinetic study and thermal decomposition behavior of viscoelastic memory foam. Energy Convers Manag 119, 327–337. https://doi.org/10.1016/J.ENCONMAN.2016.04.048.

Garrido, M.A., Font, R., Conesa, J.A., 2017. Pollutant emissions from the pyrolysis and combustion of viscoelastic memory foam. Sci. Total Environ. 577, 183–194. https://doi.org/10.1016/J.SCITOTENV.2016.10.159.

Griffiths, T., Coe, C., Fiori, F., Berry, I., 2013. Mattress Recycling. Waste and Resource Management 166, 158–166. https://doi.org/10.1680/WARM.12.00011.

Guo, X., Wang, L., Zhang, L., Li, S., Hao, J., 2014. Nitrogenous emissions from the catalytic pyrolysis of waste rigid polyurethane foam. J. Anal. Appl. Pyrol. 108, 143–150. https://doi.org/10.1016/j.jaap.2014.05.006.

Hawley, J.M., 2014. Textile Recycling, in: Handbook of Recycling: State-of-the-Art for Practitioners, Analysts, and Scientists. Elsevier, pp. 211–217. DOI: 10.1016/B978-0-12-396459-5.00015-5.

Jiang, L., Berto, F., Zhang, D., 2021. Pyrolysis Kinetics and Flammability Evaluation of Rigid Polyurethane with Different Isocyanate Content. Molecules 2021, Vol. 26, Page 2386 26, 2386. DOI: 10.3390/MOLECULES26082386.

Jomaa, G., Goblet, P., Coquelet, C., Morlot, V., 2015. Kinetic modeling of polyurethane pyrolysis using non-isothermal thermogravimetric analysis. Thermochim Acta 612, 10–18. https://doi.org/10.1016/J.TCA.2015.05.009.

Kale, S., 2020. The mattress landfill crisis: how the race to bring us better beds led to a recycling nightmare. The Guardian.

Ketata, N., Sanglar, C., Waton, H., Alamercery, S., Delolme, F., Raffin, G., Grenier-Loustalot, M.F., 2005. Thermal degradation of polyurethane bicomponent Systems in Controlled Atmospheres. Polym. Polym. Compos. 13 https://doi.org/10.1177/096739110501300101.

Li, C.Z., Tan, L.L., 2000. Formation of NOx and SOx precursors during the pyrolysis of coal and biomass. Part III. further discussion on the formation of HCN and NH3 during pyrolysis. Fuel 79, 1899–1906. https://doi.org/10.1016/S0016-2361(00)00008-9.

Mehta, R., Golkaram, M., 2022. Sustainability Evaluation of Pyrolysis of Waste Mattresses: A Comparison with Alternative End-of-Life Treatments, in: Albrecht, S., Fischer, M., Scagnetti, C., Barkmeyer, M., Braune, A. (Eds.), E3S Web of Conferences. p. 01001. DOI: 10.1051/e3sconf/202234901001.

Niu, M., Xin, L., Cheng, W., Liu, S., Wang, B., Xu, W., 2023. Effects of pressurized pyrolysis on the chemical and porous structure evolution of coal Core during deep

underground coal gasification. ACS Omega 8, 40153–40161. https://doi.org/10.1021/ACSOMEGA.3C03327/ASSET/IMAGES/LARGE/AO3C03327_0013.JPEG.
Serrano, D., Horvat, A., Batuecas, E., Abelha, P., 2022. Waste tyres valorisation through gasification in a bubbling fluidised bed: an exhaustive gas composition analysis. Renew. Energy 200, 1438–1446. https://doi.org/10.1016/J.RENENE.2022.10.025.
Shudo, T., Nagano, T., Robavashi, M., 2003. Combustion characteristics of waste-pyrolysis gases in an internal combustion engine. Int. J. Automot. Technol. 4, 1–8.
Veksha, A., Chen, W., Liang, L., Lisak, G., 2022. Converting polyolefin plastics into few-walled carbon nanotubes via a tandem catalytic process: importance of gas composition and system configuration. J. Hazard. Mater. 435, 128949 https://doi.org/10.1016/J.JHAZMAT.2022.128949.
Veksha, A., Lu, J., Tsakadze, Z., Lisak, G., 2023. Carbon dioxide capture from biomass pyrolysis gas as an enabling step of biogenic Carbon nanotube synthesis and hydrogen recovery. ChemSusChem 16, e202300143.
Veses, A., Sanahuja-Parejo, O., Martínez, I., Callén, M.S., López, J.M., García, T., Murillo, R., 2021. A pyrolysis process coupled to a catalytic cracking stage: a potential waste-to-energy solution for mattress foam waste. Waste Manag. 120, 415–423. https://doi.org/10.1016/J.WASMAN.2020.09.052.
Wan, H., Huang, Z., 2022. Pyrolysis evaluation of tennis string polyurethane and water-borne polyurethane wastes through isoconversional kinetic analysis. Polymers (basel) 14, 1501. https://doi.org/10.3390/POLYM14081501/S1.
Wang, N., Chen, D., Arena, U., He, P., 2017. Hot char-catalytic reforming of volatiles from MSW pyrolysis. Appl. Energy 191, 111–124. https://doi.org/10.1016/J.APENERGY.2017.01.051.
Wang, P.-S., Chiu, W.-Y., Chen, L.-W., Denq, B.-L., Don, T.-M., Chiu, Y.-S., 1999. Thermal degradation behavior and flammability of polyurethanes blended with poly (bispropoxyphosphazene). Polym. Degrad. Stab. 66, 307–315. https://doi.org/10.1016/S0141-3910(99)00070-1.
Zakharyan, E.M., Maksimov, A.L., 2022. Pyrolysis of polyurethanes. process features and composition of reaction products. Russ. J. Appl. Chem. 95, 191–255. https://doi.org/10.1134/S1070427222020033.
Zhang, Y., Xia, Z., Huang, H., Chen, H., 2009a. A degradation study of waterborne polyurethane based on TDI. Polym. Test. 28, 264–269. https://doi.org/10.1016/J.POLYMERTESTING.2008.12.011.
Zhang, Y., Xia, Z., Huang, H., Chen, H., 2009b. Thermal degradation of polyurethane based on IPDI. J. Anal. Appl. Pyrol. 84, 89–94. https://doi.org/10.1016/J.JAAP.2008.11.008.
Zia, K.M., Bhatti, H.N., Ahmad Bhatti, I., 2007. Methods for polyurethane and polyurethane composites, recycling and recovery: a review. React. Funct. Polym. 67, 675–692. https://doi.org/10.1016/j.reactfunctpolym.2007.05.004.